

## Application of tuned liquid dampers in controlling the torsional vibration of high rise buildings

Andrew S. Ross<sup>1a</sup>, Ashraf A. El Damatty<sup>\*1</sup> and Ayman M. El Ansary<sup>1,2b</sup>

<sup>1</sup>Department of Civil and Environmental Engineering, Western University, London, Ontario, Canada

<sup>2</sup>Faculty of Engineering, Alexandria University, Alexandria, Egypt

(Received February 23, 2015, Revised July 28, 2015, Accepted August 19, 2015)

**Abstract.** Excessive motions in buildings cause occupants to become uncomfortable and nervous. This is particularly detrimental to the tenants and ultimately the owner of the building, with respect to financial considerations. Serviceability issues, such as excessive accelerations and inter-story drifts, are more prevalent today due to advancements in the structural systems, strength of materials, and design practices. These factors allow buildings to be taller, lighter, and more flexible, thereby exacerbating the impact of dynamic responses. There is a growing need for innovative and effective techniques to reduce the serviceability responses of these tall buildings. The current study considers a case study of a real building to show the effectiveness and robustness of the TLD in reducing the coupled lateral-torsional motion of this high-rise building under wind loading. Three unique multi-modal TLD systems are designed specifically to mitigate the torsional response of the building. A procedure is developed to analyze a structure-TLD system using High Frequency Force Balance (HFFB) test data from the Boundary Layer Wind Tunnel Laboratory (BLWTL) at the University of Western Ontario. The effectiveness of the unique TLD systems is investigated. In addition, a parametric study is conducted to determine the robustness of the systems in reducing the serviceability responses. Three practical parameters are varied to investigate the robustness of the TLD system: the height of water inside the tanks, the amplitude modification factor, and the structural modal frequencies.

**Keywords:** vibration control; tuned liquid dampers; high-rise buildings; wind tunnel tests; sloshing motion

### 1. Introduction

Recent trends show that buildings are taller and more flexible, use lighter materials, and have innovative structural systems and less damping. This trend causes buildings to become more susceptible to dynamic loading, especially for those having complex shapes where torsion becomes an issue. A torsional sensitivity arises when a building has a complex shape, which may lead to significant aerodynamic torsion loads and also to potentially significant eccentricity between the center of mass and center of rigidity. Combining a large eccentricity with a torsional stiffness that is less than the lateral stiffness, results in dominant torsion modes. This configuration

---

\*Corresponding author, Professor, E-mail: [damatty@uwo.ca](mailto:damatty@uwo.ca)

<sup>a</sup> Structural Engineer, E-mail: [aross33@gmail.com](mailto:aross33@gmail.com)

<sup>b</sup> Assistant Professor, E-mail: [aelansa@uwo.ca](mailto:aelansa@uwo.ca)

leads to excessive motions when strong winds or earthquakes dynamically excite the building. To mitigate the motions to an acceptable level, the implementation of an auxiliary damping system is necessary. One of the effective passive dynamic vibration absorbers (DVA) is the tuned liquid damper (TLD), which modifies the frequency response characteristics of the structure.

A TLD is a rigid tank partially filled with a liquid, usually water. The TLD sloshing frequency is tuned to the frequency of a specific mode of the structure that requires control. During dynamic excitation, the liquid will slosh against the walls of the tank. This sloshing motion imparts inertial forces approximately anti-phase to the dynamic excitation, thus reducing the structural motion. The advantages of using tuned liquid dampers (TLDs) are that they have low installation and maintenance costs, have an easily adjustable tuning frequency, can operate under a wide range of excitation amplitudes, and are applicable for existing structures. A disadvantage is that space requirements can be high in order to achieve an adequate mass of water.

The first damper utilizing liquid sloshing to dissipate energy was a nutation damper, which is a disc shaped container (Modi *et al.* 1990). Kareem (1990) applied the same energy dissipation concept to a rectangular tank called a tuned sloshing damper (TSD), which is generally much larger than a nutation damper. However, the inherent damping through viscous dissipation in the boundary layers of the liquid in the TSD is an order of magnitude less than optimal. Research has shown that using lattice screens will increase the inherent damping to an optimal level (Fediw *et al.* 1995, Warnitchai and Pinkaew 1998). This modern form of the TLD introduces a complex liquid motion through the screens that requires difficult computation to predict the sloshing behaviour. Appropriate linearization assumptions were made to develop a technique to transform the TLD into an equivalent tuned mass damper (TMD), as a means to simplify the analysis (Sun *et al.* 1995). The technique equates the energy dissipation of the tuned liquid damper to an equivalent single degree-of-freedom (SDOF) TMD at specific amplitude of excitation. The nonlinear TLD properties vary with the excitation amplitude; therefore, the TLD is represented as an SDOF with an amplitude-dependent set of equivalent TMD properties. Despite the dependency on amplitude, a TLD remains effective over a wide range of excitations, varying from small (wind) to large (earthquake) (Reed *et al.* 1998).

Tait *et al.* (2005a) developed a sophisticated numerical model to predict the sloshing motion of the TLD equipped with slat screens. Using this numerical model, Tait *et al.* (2004a) developed an improved equivalent TMD method to determine the amplitude-dependent properties of a TLD equipped with slat screens. Furthermore, Tait *et al.* (2004b) demonstrated that a TLD is an effective and robust DVA for one-dimensional excitation. Tait *et al.* (2005b) extended the same conclusions for a TLD designed to dissipate energy in two orthogonal directions.

Despite previous research conducted on tuned liquid dampers, the practical application of this technique has been limited to reducing the lateral motion of buildings. In terms of serviceability criteria, the torsional vibration of a building can cause excessively high corner accelerations and displacements. Tuned mass dampers (TMDs) have been demonstrated to reduce the torsional behaviour of buildings when they are placed away from the center of rigidity, thereby acting as an eccentric mass that works against the motion of the building (Singh *et al.* 2002, Tse *et al.* 2007, Ueng *et al.* 2008, Xu *et al.* 1992). A TMD behaves similarly to a TLD by means of exerting an inertial force that opposes the motion; therefore, a TLD should also be capable of reducing torsional motions. In this paper, a case study is considered to show the ability of a TLD system to reduce the lateral-torsional coupled motion of a building.

Previous research has shown that using a multiple tuned liquid damper (MTLD) with a distributed tuning ratio over a range of frequencies around the fundamental structural frequency

leads to a more effective and robust system (Rahman 2007). Li *et al.* (2004) extended this concept to tuning the TLD or TMD system to multiple structural modal frequencies, which is especially useful for closely spaced fundamental frequencies. To achieve an optimized system, previous studies have shown that it is advisable to employ dampers that are tuned to the first few dominant modes of the building (Koh *et al.* 1995). The current study is conducted on an irregular high-rise building where several coupled lateral-torsional modes contribute to the response of the building; therefore, the concept of suppressing multiple modes by means of a TLD system is implemented. The building was tested at the Boundary Layer Wind Tunnel Laboratory (BLWTL) at the University of Western Ontario using the high frequency force balance (HFFB) technique. The results proved that the building exceeds serviceability criteria; therefore, the impetus of the research came from the need to reduce the top floor accelerations to an acceptable level. Three unique TLD systems (each with different water masses) are designed for the building. The structure-TLD systems are subjected to wind loading from the BLWTL data and are numerically solved to demonstrate the ability of the TLD system to reduce the structural motion. The best system is then chosen for a parametric study. Three practical parameters are varied to investigate the robustness of the TLD system: the height of water inside the tanks, the amplitude modification factor, and the structural modal frequencies. It should be mentioned that the structural modal frequencies are considered in the parametric study because the as-built structural frequencies might deviate from the frequencies estimated from a computer model by over  $\pm 15\%$  (Li *et al.* 2007). The amplitude modification factor is introduced in the numerical model to calculate the physical displacement experienced by the TLD system from the combined lateral-torsional movement.

## 2. Description of the tested building

A 50-storey irregular reinforced concrete building with a height of 161.7 meters is considered in this study. The building has an L-shaped floor plan, which introduces a significant eccentricity between the center of mass and the center of rigidity, thereby presenting a torsional sensitivity. The lateral load resisting elements are shear walls, primarily near the center of the floor plan, and moment resisting frames, located along two exterior faces of the building. This exacerbates the torsional sensitivity because the torsional stiffness is significantly lower than the lateral stiffness. The stiffness disparity and non-coinciding center of mass and center of rigidity lead to highly coupled lateral-torsional action.

The coupled action is confirmed from a modal analysis conducted on the building to investigate the fundamental vibration characteristics. Fig. 1 illustrates the first three vibration mode shapes that have corresponding periods of 6.30, 5.30, and 3.78 seconds. The torsion mode shapes are multiplied by the overall radius of gyration (13.2m) of the building to maintain dimensional consistency with the sway mode shapes. In other words, this technique allows for relative comparison of the mode shapes in the three principle directions. The first mode displays strong coupling action in the  $X$  and  $\theta$  directions. Similarly, the building exhibits coupled action in the  $Y$  and  $\theta$  directions torsion for the second mode.

The mode shapes are transformed from the center of masses (CM) to the center of coordinates (CC) as a means to align the building with the point where the HFFB measurements are recorded. In addition, this technique helps in linearizing the mode shapes (Tse *et al.*, 2009) and assembling the lumped masses on a single vertical axis, which simplifies the analysis of the building. The

mode shapes at the CC are equal to

$$\begin{Bmatrix} \varphi_{xi} \\ \varphi_{yi} \\ \varphi_{\theta i} \end{Bmatrix}_{\text{coordinate}} = \begin{bmatrix} 1 & 0 & e_{yi} \\ 0 & 1 & -e_{xi} \\ 0 & 0 & 1 \end{bmatrix} \begin{Bmatrix} \varphi_{xi} \\ \varphi_{yi} \\ \varphi_{\theta i} \end{Bmatrix}_{\text{mass}} \quad (1)$$

where the new mass matrix must satisfy

$$[m]_{\text{mass}}\{\varphi^2\}_{\text{mass}} = [m]_{\text{coordinate}}\{\varphi^2\}_{\text{coordinate}} \quad (2)$$

The generalized quantities used for analysis are not altered by the transformation of the reference axes from the CM to the CC (Yip, 1995). Fig. 2 illustrates the location of the CC and the sign conventions used in the analysis.

The generalized properties of the building, which are used in the analysis, are calculated using the mode shapes in Fig. 1 and are summarized in Table 1. The exact value of structural damping ratio in the building is generally not known, particularly in the design stage. In order to bracket the range of possible responses, it is important to use a range of possible damping ratios in the initial analysis. This provides a range of required damping from the auxiliary device so the device can be designed such that it will be in the tunable range once the structural damping ratio is determined after the building is completed. The initial analyses were carried out for two different levels of damping ratios – one and two percent.

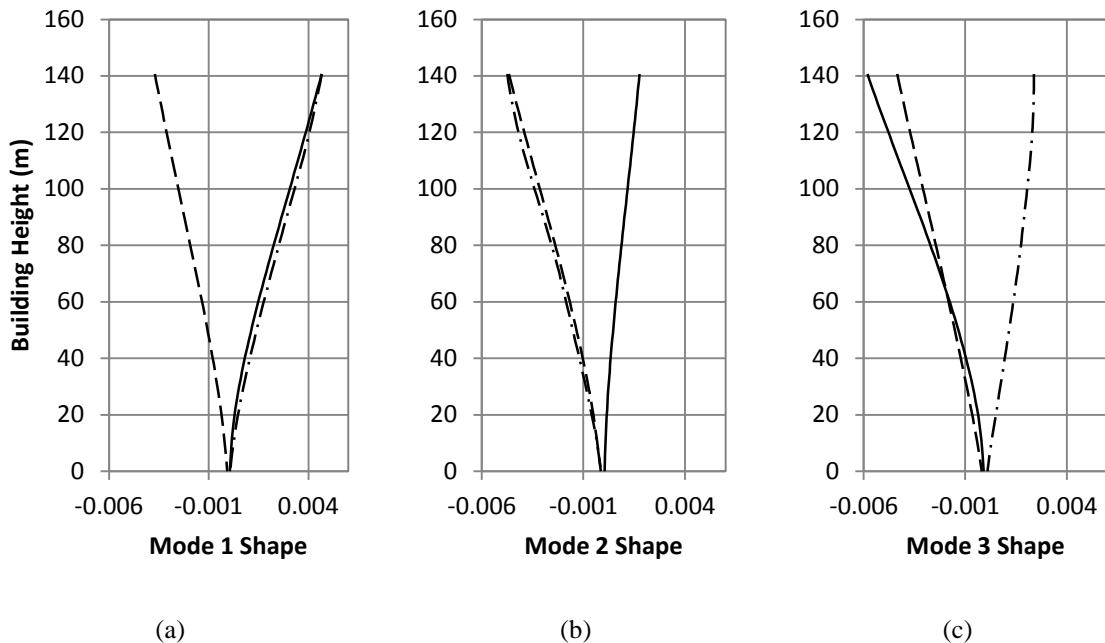


Fig. 1 The mode shapes for sway in the X direction (solid line), sway in the Y direction (dashed line), and torsion (dash-dot line) for (a) mode 1, (b) mode 2, and (c) mode 3.

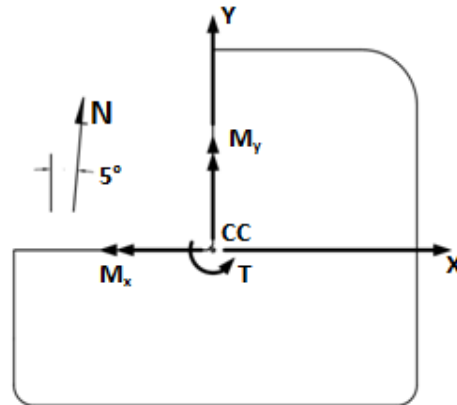


Fig. 2 The building floor plan illustrating the center of coordinates and the sign convention

Table 1 The modal frequencies and generalized properties for the first three modes of the building

Mode $j$	$f_j$ (Hz)	$m_j^*$ (kg)	$k_j^*$ (N/m)	$c_j^*$ (kg/s) (1%)	$c_j^*$ (kg/s) (2%)
1	0.1588	988.8	984.0	19.7	39.5
2	0.1887	983.6	1383.2	23.3	46.7
3	0.2645	978.1	2700.9	32.5	65.0

### 3. Response of the building to wind loading

The motions due to twisting moments can be particularly disturbing to occupants in a high-rise building. To check the comfort levels of a torsionally sensitive building, wind tunnel testing is required to predict the response under serviceability wind loads corresponding to 5 or 10 years return period. The performance of the building is evaluated using the high frequency force balance (HFFB) testing technique at the Boundary Layer Wind Tunnel Laboratory (BLWTL) at the University of Western Ontario. Rigid lightweight foam is used to produce a model of the building with a geometric length scale of 1:400. The model is mounted on a balance, which is capable of recording the base shear forces, bending moments, and torque. The HFFB testing technique sufficiently predicts the torsional response and accommodates 3D coupled mode shapes (Tschanz 1982, Yip and Flay 1995).

The main advantage of the HFFB technique is the capacity to predict the generalized wind force (GWF),  $F_j^*(t)$ , directly from the measured base overturning and torsional moments. The GWF takes the form shown in Eq. (3)

$$F_j^*(t) = a_{xj} \frac{1}{H} C_{xj} M_x(t) + a_{yj} \frac{1}{H} C_{yj} M_y(t) + 0.7 a_{\theta j} C_{\theta j} M_{\theta}(t) \quad (3)$$

where  $M_{\gamma}(t)$  is the time-dependent base moment for direction  $\gamma$  (where  $\gamma = x, y, \theta$ ) recorded from the HFFB test and scaled by the design wind speed and model length scale. In the formulation of the GWF, the assumption is made that the mode shapes are linear in the sway

directions and constant in the torsional direction; therefore, mode shape correction factors,  $C_{\gamma j}$ , are applied to the base moments to linearize the mode shapes for direction  $\gamma$ . Table 2 shows the correction factors, based on simplified representation of the mode shape and the mean wind speed profile using power law formulation (Lam and Li 2009). However, the same simplified mean wind speed profile is applied to both sides to determine the correction ratio, the effect of its variation on the correction factor is minimal, thus is generally ignored (Zhou *et al.* 1999b). Furthermore, the base torsional moment requires an empirical correction of 0.7 to transform the mode shape from linear to constant. For 3D coupled mode shapes, the relative contributions from each direction are accounted for by applying modal mixing factors,  $a_{\gamma j}$  (Yip and Flay 1995). The modal mixing factors are equal to the mode shape value at the CC of the top floor.

HFFB tests were conducted every 10 degrees of azimuth and at a few other critical wind directions with various wind exposures for a total of 43 tests. Surrounding buildings were modeled within a 550-meter radius and cubic roughness elements were raised upwind of the model. Each test lasted 250 seconds (approximately 4 hours in full-scale) and data were sampled at a rate of 116 hertz. The meteorological wind climate model is applied to this data to give the full-scale base shears and moments. The site-specific wind climate model for the building in this study predicts a mean hourly wind speed of 41.7 m/s at 500 meters for a 10-year return period – the return period for serviceability responses. Using this model, the GWF for the first three structural modes is calculated and a portion (10-minute portion) is shown in Fig. 3 for the 245 degrees of azimuth wind direction.

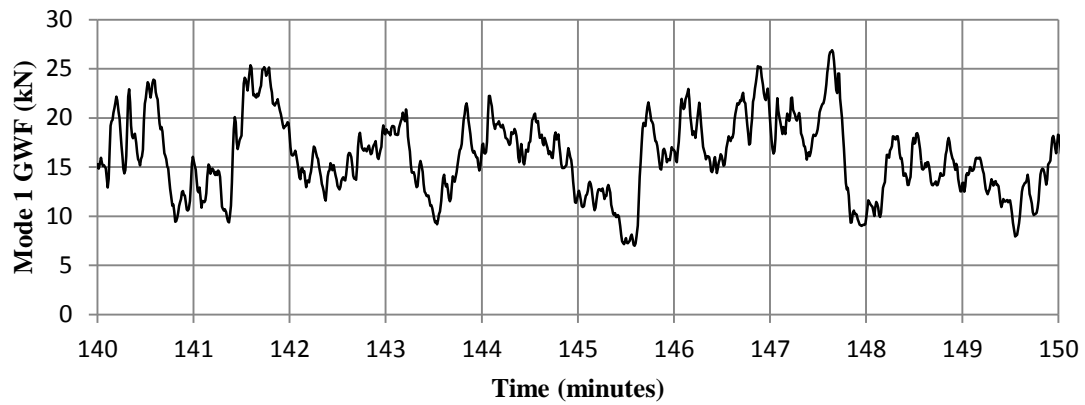
Classical modal analysis is used to solve the responses of the building subjected to the GWF. The structural modes are decoupled and solved independently by using the generalized properties of the building and GWF for mode  $j$ . Fundamentally, the building is transformed into an SDOF system described by

$$m_j^* \ddot{\xi}_{sj}(t) + c_j^* \dot{\xi}_{sj}(t) + k_j^* \xi_{sj}(t) = F_j^*(t) \quad (4)$$

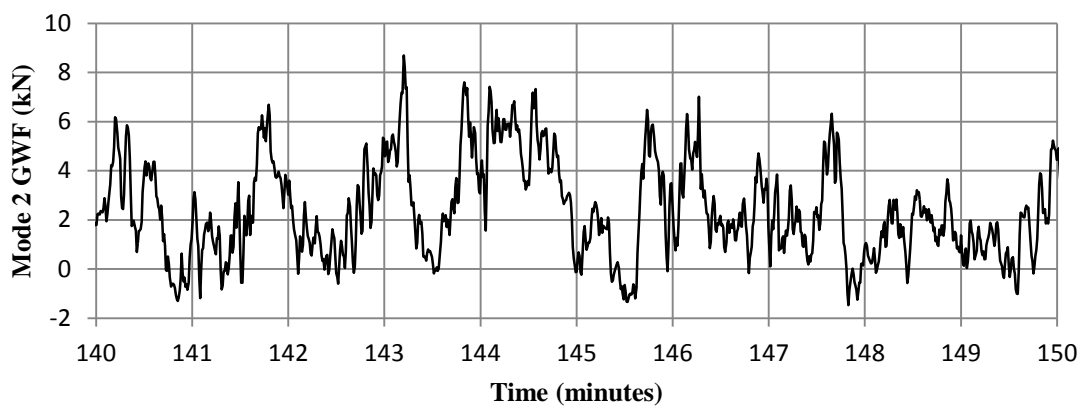
where  $\ddot{\xi}_{sj}$ ,  $\dot{\xi}_{sj}$ , and  $\xi_{sj}$  are the generalized acceleration, velocity, and displacement responses of the structure. The equation of motion is solved in the time domain using the fourth-order Runge-Kutta-Gill numerical method to obtain the modal generalized responses, which are transformed to the physical modal responses by use of the mode shapes. The modal responses are combined through summation. From the time series for each response, the Lieblein BLUE technique is employed for the determination of the statistical parameters of a Type I extreme-value distribution (Lieblein 1974). The technique provides a probabilistic model, thus resulting in a more controlled and accurate prediction of the peak responses of the building. Additionally, the probability distribution accommodates the calculation of 1-hour peak responses for a given confidence interval.

Table 2 The correction factors for the nonlinear mode shapes

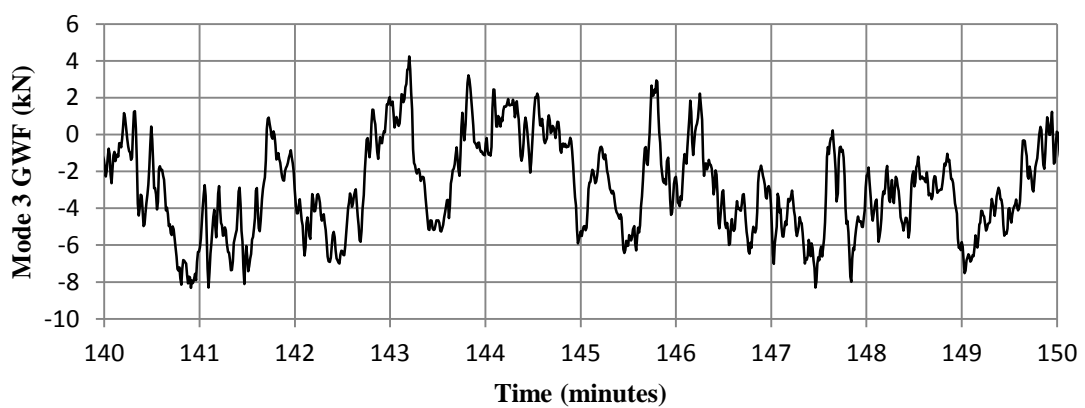
Mode $j$	$C_{xj}$	$C_{yj}$	$C_{\theta j}$
1	0.91	0.96	0.99
2	0.92	0.96	1.02
3	0.90	1.01	1.40



(a)



(b)



(c)

Fig. 3 A 10-minute segment of the generalized wind force at a  $245^\circ$  angle of incidence for (a) mode 1, (b) mode 2, and (c) mode 3

The 43 tests are solved in this manner and combined by response-specific importance factors,  $\beta(\alpha)$ . These factors describe the relative importance of each wind angle tested and are calculated from the site-specific wind climate model obtained from the BLWTL. The factors sum to unity. The result is a peak and root-mean-square (RMS) response variable for each serviceability limit issue as shown in Table 3 for a 1% and 2% damping ratio. The response variables are determined using a computer numerical model developed specifically for this study. The RMS response is a measure of the variance in the response variable and provides insight into the degree of fluctuation of the response.

The accelerations are calculated at the uppermost occupied floor ( $z = 140.7$  m) and are expressed in terms of the gravitational acceleration (milli-g). The torsional acceleration is calculated using a lever arm of 23.0 meters – the furthest occupiable distance from the CC. The centroidal acceleration is the maximum combined acceleration at the CC. The corner acceleration is the absolute maximum acceleration experienced from the collection of the five corners of the floor plan. The deflections are calculated at the top of the building ( $z = 161.7$  meters) and the lever arm for the torsional deflection is 24.0 meters.

The magnitudes of the peak torsional acceleration are much greater than the peak lateral acceleration, which clearly demonstrate the torsional irregularity of the building. The torsion acceleration manifests itself as large additional translational component as the distance away from the CC increases, thereby causing the combined accelerations to exceed recommended limits. Criteria for acceptable wind-induced motions are related to human perception thresholds, which are calculated using a probabilistic approach and experimental evaluation. Based on this concept, the BLWTL has recommended the following criteria for acceptable accelerations: 10 to 15 milli-g for residential buildings, 15 to 20 milli-g for hotels, and 20 to 25 milli-g for office buildings (Isyumov 1994). In addition to the excessive building accelerations, the torsional velocity exceeds the recommended maximum of 5 milli-rad/s.

Table 3 The peak and RMS serviceability responses of the building

Response Variable	1% Damping		2% Damping	
	Peak	RMS	Peak	RMS
<b>X Acceleration (milli-g)</b>	17.1	7.4	12.2	5.2
<b>Y Acceleration (milli-g)</b>	17.1	7.4	12.2	5.2
<b>Torsional Acceleration (milli-g)</b>	31.6	13.4	21.6	9.2
<b>Centroidal Acceleration (milli-g)</b>	19.8	5.1	14.3	3.6
<b>Corner Acceleration (milli-g)</b>	35.4	9.6	25.5	6.8
<b>Torsional Velocity (milli-rad/s)</b>	11.5	5.3	8.2	3.6
<b>X Deflection (mm)</b>	288	82	258	65
<b>Y Deflection (mm)</b>	277	84	252	69
<b>Torsional Deflection (mm)</b>	481	146	411	110

#### 4. Description of tuned liquid dampers

To ensure the building responses remain below the perception threshold, the use of a DVA is necessary to increase the damping. Tuned liquid dampers are chosen because they reach peak efficiency in the peak acceleration range of 12 to 22 milli-g, corresponding to a once in 10-year exceedance (Tait *et al.* 2008b). Therefore, a properly designed TLD system is an optimal DVA for the building in this study.

The tuning ratio and mass ratio are important parameters that strongly influence the performance of the TLD. They both depend on the tank length,  $L_w$ , width,  $b_w$ , and water height,  $h_w$ , shown in Fig. 4 along with the placement of the damping screens. The tuning ratio,  $\Omega$ , is defined as the ratio of the sloshing frequency to the structural frequency in the mode that the dynamic motions are to be suppressed. The mass ratio,  $\mu$ , is defined as the ratio of the generalized participating water mass to the structural generalized mass. The ratios take the following form

$$\Omega = \frac{f_w}{f_s} \tag{5}$$

$$\mu = \frac{\alpha_p M_p}{m^*} \tag{6}$$

where  $\alpha_p$  is the proportion of water mass that contributes to the fundamental sloshing mode of the TLD defined by Eq. (8) and  $m^*$  is the generalized mass of the building for the desired mode.  $M_p$  is the total generalized water mass defined by Eqs. (9) and (10). Despite the amplitude-dependent nonlinear behaviour of a TLD, the use of linear wave theory to estimate the water sloshing frequency,  $f_w$ , and potential flow theory to estimate the water mass contributing to the fundamental sloshing mode,  $m_1$ , are acceptable for the initial design (Tait *et al.* 2005a). These estimations take the form

$$f_w = \frac{1}{2\pi} \sqrt{\frac{\pi g}{L_w} \tanh\left(\frac{\pi h_w}{L_w}\right)} \tag{7}$$

$$\alpha_p = \frac{m_1}{m_w} = \frac{8 \tanh\left(\frac{\pi h_w}{L_w}\right)}{\pi^3 \left(\frac{h_w}{L_w}\right)^3} \tag{8}$$

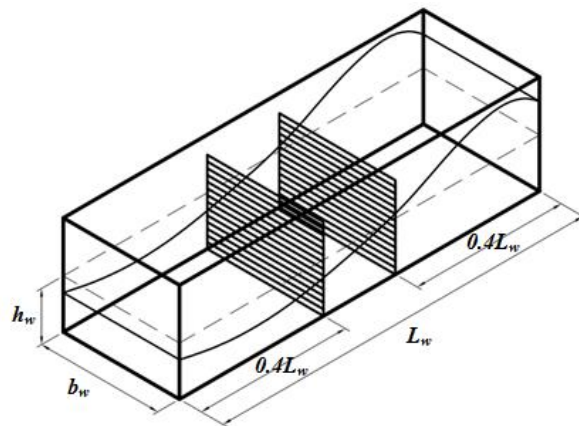


Fig. 4 A diagram of a typical rectangular TLD showing the dimensions and the screen locations

where  $g$  is the acceleration of gravity and  $m_w$  is the total mass of water in a single tank. An optimal TLD design is promoted by setting the tuning ratio to near unity and mass ratio to within a range of one to four percent (Tait 2008a).

To characterize the nonlinear properties of a TLD, an equivalent amplitude-dependent tuned mass damper (TMD) approach is used (Sun *et al.* 1995). The concept involves matching the energy dissipation of the sloshing water to the energy dissipation of an equivalent TMD for specific excitation amplitudes. The result is the TLD described by a frequency,  $f_{TLD}$ , mass,  $m_{TLD}$ , and damping ratio,  $\zeta_{TLD}$ , which are dependent on the amplitude. Depending on the tank dimensions, these parameters are expressed as linear or power functions, which increase as the amplitude increases (Tait *et al.* 2004a).

#### 4.1 Unique designs for coupled motion

Three TLD systems are designed specifically for coupled lateral-torsional motion and are shown in Fig. 5. They are denoted as TS-1, TS-2, and TS-3. The main difference between the three systems is the TLD mass ratio, which ranges from 1.28 to 4.94 percent. This is achieved by increasing the size and number of tanks. Furthermore, the TLD system layouts are chosen to capture a wide range of TLD mass ratios such that TS-2 has a TLD mass ratio approximately twice that of TS-1 and two-thirds that of TS-3. This allows for investigation of the effect of the TLD mass ratio on the building response. TS-1 uses 1D tanks, TS-2 utilizes 2D tanks, and TS-3 employs two layers of 1D tanks. Tamura *et al.* (1996) demonstrated the effective use of floor space for multiple layers of TLDs in airport control towers, located in Japan. The 2D tanks are designed as two independent 1D tanks because the wave motions and base shear forces in the tanks are uncoupled in the two principle orthogonal directions (Tait *et al.* 2007).

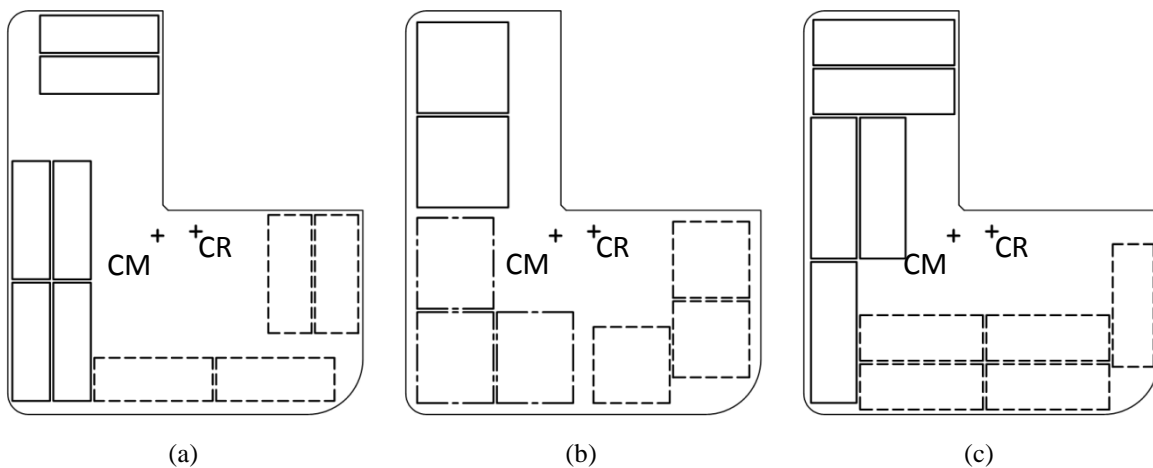


Fig. 5 The layout of the TLDs tuned to mode 1 (solid line), mode 2 (dashed line), and both mode 1 and 2 (dash-dot line) for (a) TS-1, (b) TS-2, and (c) TS-3

The three TLD systems are designed for installation on the roof ( $z = 140.7$  meters) of the building. Fig. 1 illustrates that the first two modes have a high torsional contribution to the dynamic response. To improve the effectiveness of the vibration control, the first several modes should be controlled by TLDs (Li *et al.* 2004); therefore, each of the three TLD systems will have two sets of tanks – one set tuned to mode 1 and a second set tuned to mode 2. Note that TS-2 has a set of tanks tuned to both mode 1 and mode 2. To maximize the amplitude experienced by the TLD, the tanks are placed around the perimeter of the floor plan. This also increases the generalized water mass by introducing an eccentricity,  $L_x$  or  $L_y$ , between the tanks and the center of mass of the building. The generalized water mass for a single tank aligned in the X or Y direction, respectively, is calculated by

$$m_{p,i} = m_w (\varphi_{x,i} + L_{y,i} \varphi_{\theta,i})^2 \quad (9)$$

$$m_{p,i} = m_w (\varphi_{y,i} - L_{x,i} \varphi_{\theta,i})^2 \quad (10)$$

where  $\varphi_{\gamma,i}$  is the mode shape value at the TLD level for direction  $\gamma$  for mode  $i$ . The summation of the generalized water mass,  $M_p$ , of the tanks for each system is shown in Table 4 for mode 1 and mode 2. Note that the ratio of the total water mass,  $M_w$ , to the structure mass,  $m_s$ , for TS-3 is similar to TS-2 but the TLD mass ratio,  $\mu$ , is much greater for TS-3 because the floor plan space is used more effectively – the tanks of TS-3 have a greater eccentricity,  $L_x$  and  $L_y$ . The main difference between the designs is the generalized water mass, which consequently affects the TLD mass ratio,  $\mu$ . The TLD system layouts are chosen to capture a wide range of TLD mass ratios such that TS-2 has a TLD mass ratio approximately twice that of TS-1 and two-thirds that of TS-3. This allows for investigation of the effect of the TLD mass ratio on the building response.

The sloshing frequency is directly related to the tank dimensions. The length and height of the tank are chosen to achieve a value of unity for the tuning ratio. Table 4 shows the dimensions chosen for the three systems along with the corresponding sloshing frequency. The height to length ratio is limited to a maximum of 0.2 to ensure the validity of the shallow water wave theory. Conversely, the ratio is kept sufficiently high to reduce the space requirements, the nonlinearity of the sloshing motion, and the potential wave breaking action inside the tank (Tait *et al.* 2005a). Moreover, the nonlinear response characteristics increase as the water depth to tank length ratio is reduced (Tait *et al.* 2004a).

The use of damping screens in the tanks is important to increase the inherent damping of the TLD. Without screens, the inherent damping relies on viscous dissipation in the boundary layers at the walls and bottom of the tank and from free surface contamination. This results in an inherent damping that is significantly less than optimal (Fediw *et al.* 1995). To achieve the effective optimal damping ratio shown in Table 4, this study uses slat screens in all the tanks. Two screens, with a solidity ratio of 0.42, placed at the  $0.4L_w$  and  $0.6L_w$  locations provide a near optimal inherent damping. The utilization of damping screens also reduces the nonlinearity of the TLD by removing the higher sloshing harmonics, and reducing the maximum wave height, thus reducing the chance of wave breaking for any given amplitude of excitation (Tait *et al.* 2005a). Wave breaking will occur approximately when the water at the end walls reaches a height of  $2h_w$  (Sun and Fujino 1994).

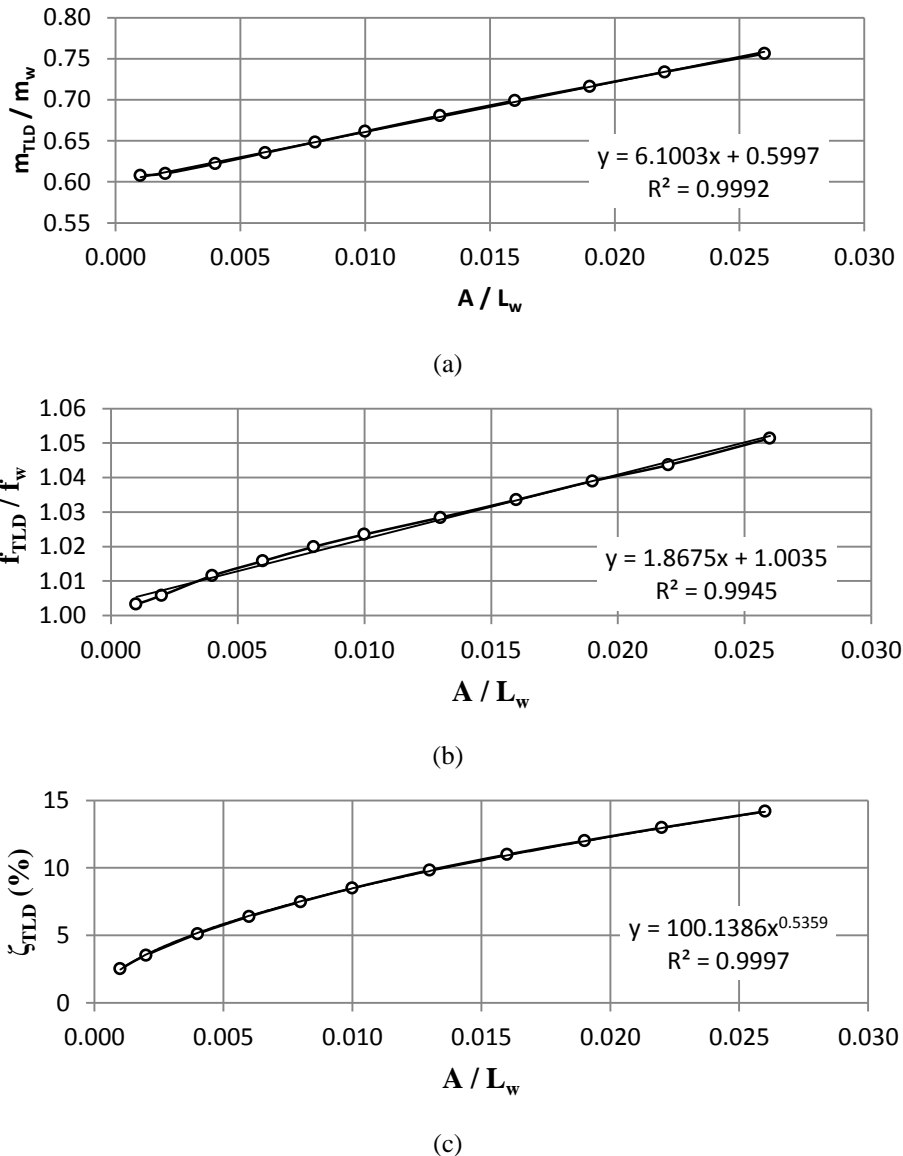


Fig. 6 The TLD (a) mass ratio, (b) frequency ratio, and (c) damping ratio with respect to the normalized amplitude of excitation for the mode 1 tanks of TS-3

Using a numerical model developed by Tait *et al.* (2004a), a set of amplitude-dependent TLD properties are evaluated. The program performs discrete frequency sweep tests on the TLD at a desired amplitude of excitation,  $A$ , to produce an equivalent TMD frequency, mass, and damping ratio. The three amplitude-dependent properties for mode 1 tanks of TS-3 are shown in Fig. 6 with a fitted curve and the corresponding  $R^2$  value. The  $R^2$  value describes how well the curve fits the data points (unity is a perfect fit). A unique set of these properties are determined for each mode of the three TLD systems and are used in the response evaluation of the structure-TLD system.

### 5. Response of the Building with a TLD System

#### 5.1 Structure-TLD numerical model

Tait *et al.* (2004b) formulated a method to analyze the complex structure-TLD system with the TLD tuned to a particular mode. Fig. 7(b) illustrates the building characterized by a generalized mass,  $m_j^*$ , stiffness,  $k_j^*$ , and damping,  $c_j^*$ , for mode  $j$ . The TLD interacts with the generalized building through a second DOF with amplitude-dependent equivalent to TMD properties as shown in Fig. 7(c). The equation of motion for the 2DOF system takes the form

$$\begin{bmatrix} m_j^* + m_o & 0 \\ 0 & m_{TLD}(A) \end{bmatrix} \begin{Bmatrix} \ddot{\xi}_s(t) \\ \ddot{\xi}_{TLD}(t) \end{Bmatrix} + \begin{bmatrix} c_j^* + c_{TLD}(A) & -c_{TLD}(A) \\ -c_{TLD}(A) & c_{TLD}(A) \end{bmatrix} \begin{Bmatrix} \dot{\xi}_s(t) \\ \dot{\xi}_{TLD}(t) \end{Bmatrix} + \begin{bmatrix} k_j^* + k_{TLD}(A) & -k_{TLD}(A) \\ -k_{TLD}(A) & k_{TLD}(A) \end{bmatrix} \begin{Bmatrix} \xi_s(t) \\ \xi_{TLD}(t) \end{Bmatrix} = \begin{Bmatrix} F_j^*(t) \\ 0 \end{Bmatrix} \tag{11}$$

where  $m_{TLD}$ ,  $k_{TLD}$ , and  $c_{TLD}$ , are the equivalent TMD mass, stiffness, and damping coefficient with respect to the amplitude,  $A$ . The excitation force is the GWF,  $F_j^*(t)$ . To account for the nonlinear dynamic properties of the TLD, the maximum displacement (or amplitude) is calculated for cycle  $n$  and is used to update the TLD mass,  $m_{TLD}$ , damping coefficient,  $c_{TLD}$ , and stiffness,  $k_{TLD}$ , for cycle  $n + 1$  using the appropriate TLD equations – similar to the equations shown in Fig. 6. However, before calculating the updated TLD properties, an amplitude modification factor (AMF),  $\Phi_j$ , is applied to the maximum displacement to transform the generalized response to a physical response. This accounts for the combined lateral-torsional motion. The AMF is calculated using a normalized weighted-average of the water mass multiplied by the mode shape value at the tank location for each TLD. Table 5 summarizes the values used in the analysis. The analysis solves the structure-TLD system for the first two modes of vibration and combines them through addition with the third mode solved as an SDOF system because there is no TLD tuned to the third mode.

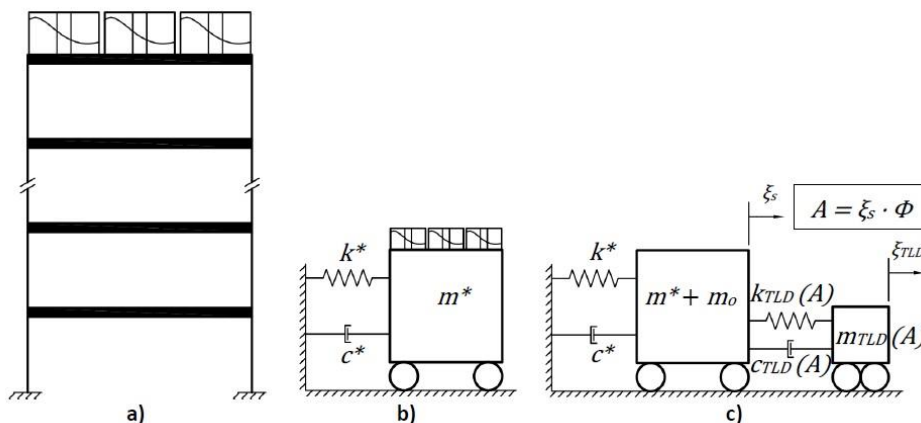


Fig. 7 The transformation of (a) the structure-TLD system into (b) a generalized structural system with TLDs then into (c) a 2DOF system

Table 5 The amplitude modification factors for each mode of the three TLD systems

	Mode $j$	$\Phi_j$
TS-1	1	0.00835
	2	0.00895
TS-2	1	0.00739
	2	0.00839
TS-3	1	0.00821
	2	0.00923

## 5.2 Performance of the building

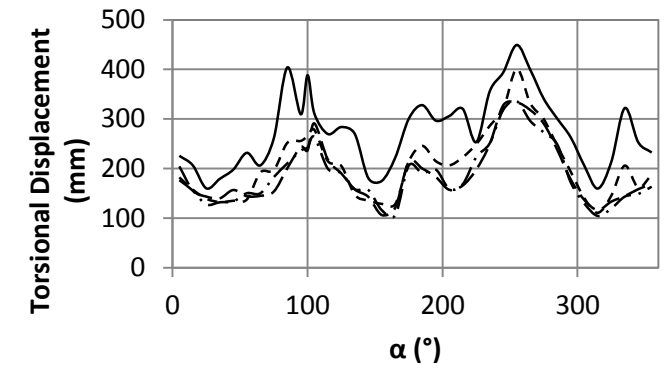
The peak and RMS building responses are solved for each of the 43 wind test angles,  $\alpha$ , in degrees of the azimuth. Figs. 8(a)-8(c) shows the peak torsional responses of the 1% damped building without a TLD system installed and with each of the three systems installed. All three TLD systems significantly reduce the peak responses of the building; however, there is only a weak disparity between the effectiveness of each TLD system. At the wind angles associated with the peak responses, the TLD systems offer a greater reduction. This demonstrates the nonlinearity of the TLD systems and the fact that a TLD is more effective when subjected to stronger motions (Tait *et al.* 2004b).

For the peak responses of the building, the site-specific wind climate model is applied to the responses for each wind direction. The probabilistic model accounts for the worst case wind direction through response-specific importance factors,  $\beta(\alpha)$ . Tables 6 and 7 show the peak hourly responses for the building with a 1% and 2% damping ratio, respectively. Both the peak and RMS responses are calculated for each TLD system along with the corresponding percent of reduction,  $\Psi$ , calculated by

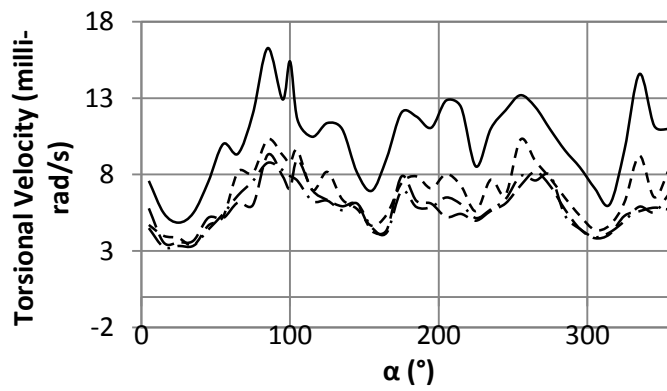
$$\Psi = \frac{R_{No\ TLD} - R_{With\ TLD}}{R_{No\ TLD}} \cdot 100 \quad (12)$$

where  $R_{With\ TLD}$  and  $R_{No\ TLD}$  are the responses with and without a *TLD* installed, respectively. The building occupants will experience significantly less motion with any one of the three *TLD* systems installed. The trend shows that as the *TLD* water mass ratio increases, the torsional responses are increasingly reduced, thus affirming that TS-3 is the most effective. However, TS-2 offers the greatest reduction in the translational responses. This occurs because the response-specific optimal *TLD* mass ratio is surpassed in the lateral direction but not reached for the torsional direction (Tait *et al.* 2004b). Furthermore, there are minimal differences in reductions between TS-2 and TS-3, thereby indicating that there is an upper limit on the optimal water mass ratio.

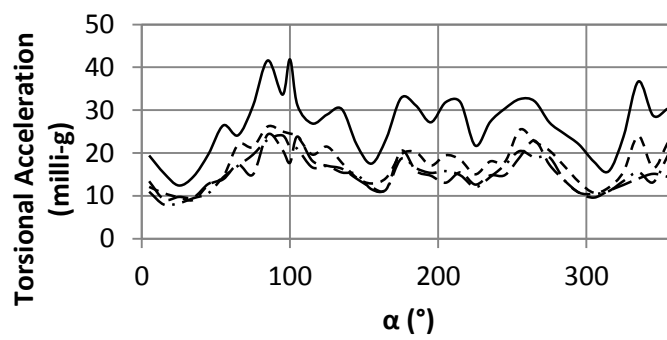
The *TLD* systems offer the greatest reduction for the torsional responses because they are specifically designed to damp the torsion motion. The implementation of TS-3 will reduce the accelerations to an acceptable level (less than 20 milli-g) except for the corner acceleration for the 1% damping case. However, the corner acceleration easily meets the recommended limit for an office building. None of the three *TLD* systems is capable of reducing the torsional velocity below the 5 milli-rad/s recommendation. However, since these values are the absolute maximum at the building corner, the majority of the building occupants will not perceive the 6.5 milli-rad/s torsional velocity.



(a)



(b)



(c)

— No TLD    - - - - TS-1    - · - · TS-2    · - - · TS-3

Fig. 8 The peak torsional (a) displacement, (b) velocity, and (c) acceleration for the 1% damping building with and without the TLD systems

The responses for the 2% damped building show a further reduction from the 1% damping level; however, the torsional velocity is still slightly above the recommended limit. In general, the *TLD* systems are less effective when the building has a higher damping ratio because the *TLD* effective damping is negatively dependent on the structural damping (Tait *et al.* 2004b). Nonetheless, a well-designed *TLD* system is an effective *DVA* for multi-modal coupled lateral-torsional motion.

The RMS values are included to demonstrate the ability of the *TLD* systems to reduce the fluctuations of the building motion. The *TLD* systems are capable of reducing the RMS values more significantly than the peak responses. The *TLD* system essentially reduces the cyclical swaying and twisting of the building to levels that are significantly less perceptible than without the *TLD* system. There is still debate between whether the peak or RMS response is the best measure for serviceability limit criteria (Pagnini and Solari 1998). Regardless, a well-designed *TLD* system will significantly reduce the motion of a high-rise building.

Table 6 The peak and RMS response variables for the 1% damped building with each of the three different *TLD* systems installed

Response Variable	TS-1		TS-2		TS-3	
	Peak	RMS	Peak	RMS	Peak	RMS
<b>X Acceleration (milli-g)</b>	13.9 (19.1)	5.8 (21.3)	13.0 (23.9)	5.5 (26.2)	12.9 (25.0)	5.5 (26.7)
<b>Y Acceleration (milli-g)</b>	12.5 (26.6)	5.2 (29.1)	11.6 (32.1)	4.9 (34.2)	12.1 (29.5)	5.0 (31.8)
<b>Torsional Acceleration (milli-g)</b>	20.5 (35.2)	8.5 (36.5)	17.7 (44.0)	7.3 (45.7)	17.5 (44.7)	7.3 (45.7)
<b>Centroidal Acceleration (milli-g)</b>	14.8 (25.2)	3.8 (26.6)	13.7 (30.7)	3.5 (31.1)	13.7 (30.9)	3.6 (30.5)
<b>Corner Acceleration (milli-g)</b>	24.8 (30.1)	6.3 (34.1)	21.8 (38.6)	5.4 (43.6)	20.6 (41.9)	5.1 (46.6)
<b>Torsional Velocity (milli-rad/s)</b>	7.5 (34.6)	3.3 (36.3)	6.5 (42.9)	2.9 (45.5)	6.5 (43.5)	2.9 (44.9)
<b>X Deflection (mm)</b>	258 (10.7)	65 (20.8)	253 (12.2)	61 (25.3)	255 (11.6)	61 (25.2)
<b>Y Deflection (mm)</b>	246 (11.1)	67 (20.0)	241 (13.1)	65 (23.3)	242 (12.8)	66 (21.3)
<b>Torsional Deflection (mm)</b>	399 (17.0)	104 (28.4)	380 (20.9)	95 (35.0)	381 (20.7)	96 (34.1)

Table 7 The peak and RMS response variables for the 2% damped building

Response Variable	TS-1		TS-2		TS-3	
	Peak	RMS	Peak	RMS	Peak	RMS
<b>X Acceleration (milli-g)</b>	10.8 (11.5)	4.5 (14.1)	10.3 (15.7)	4.2 (19.0)	10.2 (16.6)	4.2 (19.6)
<b>Y Acceleration (milli-g)</b>	10.0 (18.2)	4.2 (19.2)	9.5 (22.3)	3.9 (24.1)	9.7 (21.0)	4.0 (22.0)
<b>Torsional Acceleration (milli-g)</b>	16.4 (24)	6.8 (25.8)	14.3 (33.7)	5.9 (35.6)	14.1 (34.6)	5.8 (36.5)
<b>Centroidal Acceleration (milli-g)</b>	12.1 (15.8)	3.0 (17.8)	11.2 (21.7)	2.8 (22.8)	11.1 (22.2)	2.8 (22.3)
<b>Corner Acceleration (milli-g)</b>	20.2 (20.8)	5.2 (23.2)	18.1 (28.9)	4.5 (32.9)	17.2 (32.4)	4.3 (36.3)
<b>Torsional Velocity (milli-rad/s)</b>	6.2 (24.4)	2.7 (25.0)	5.4 (33.4)	2.4 (34.2)	5.3 (35.2)	2.4 (34.2)
<b>X Deflection (mm)</b>	247 (4.1)	59 (10.1)	245 (4.8)	57 (13.3)	244 (5.3)	57 (13.1)
<b>Y Deflection (mm)</b>	239 (5.3)	63 (9.2)	235 (6.9)	61 (11.3)	236 (6.5)	62 (9.9)
<b>Torsional Deflection (mm)</b>	376 (8.4)	92 (16.1)	363 (11.5)	86 (21.5)	363 (11.7)	87 (20.9)

## 6. Parametric study

To assess the robustness of the TLD system, a parametric study is performed. TS-3 displays the performance of interest by maximizing the reduction in the torsional response of the building; therefore, the parametric study is performed on this system. Three parameters are chosen for the study: the water height inside the tank, the amplitude modification factor, and the first two modal frequencies of the building. These parameters are chosen because they are the most practical variables that affect the structure-TLD performance.

### 6.1 Effect of the water height

The water height inside the *TLD* is of utmost interest because it affects both the tuning ratio and mass ratio, which are the critical parameters of a well-designed *TLD*. Evaporation, spillage, leakage, and poor maintenance will cause the water height to fluctuate. The varying water height

will simultaneously change the sloshing frequency and water mass. Ten numerical tests are conducted, each with a different water height,  $h$ , ranging between  $\pm 25\%$  of the optimal water height,  $h_w$ . The water height is considered optimal when the tuning ratio is unity. The water height, frequency, and mass used in the ten tests are shown in Table 8 for mode 1 and mode 2.

Fig. 9 shows the influence of the water height on the peak hourly responses. The results show that even a small change in the water height yields a significant change in the reduction of the peak responses. Moreover, the torsional responses, including the corner acceleration, are more sensitive than the lateral responses mainly because the building exhibits a torsional sensitivity. However, this sensitivity to changes in the water height strictly enhances the performance of the *TLD* system because of the reasoning described in the following paragraph.

The results demonstrate that TS-3 is optimally effective at a reduced water height, approximately 15% less than the designed water height. A reduced water height will lower the sloshing frequency, which increases the effectiveness of the *TLD*. The approximate optimal tuning ratio is given by

$$\Omega_{opt} = \frac{\sqrt{1+\frac{\mu}{2}}}{1+\mu} \quad (13)$$

where  $\mu$  is the *TLD* water mass ratio (Tait, 2008a). Conversely, the TS-3 becomes ineffective when the water height is increased by 20%. This situation is extremely unlikely because water cannot be added to the tanks – water is more easily removed through evaporation, leakage, or spillage. Therefore, if the structural frequency is accurately calculated, a realistic change in water height will only have a positive influence on the structure-*TLD* system. Moreover, a substantial change in water height is unlikely to go unnoticed.

Table 8 The tests performed to analyse the effect of the water height on the structure-*TLD* response

Test ID	Mode 1					Mode 2				
	$h$ (m)	$f_w$ (Hz)	$\Omega$	$M_p$ (kg)	$\mu$ (%)	$h$ (m)	$f_w$ (Hz)	$\Omega$	$M_p$ (kg)	$\mu$ (%)
<b>WH+25</b>	2.09	0.175	1.10	68.2	5.12	2.32	0.206	1.09	82.1	5.90
<b>WH+20</b>	2.01	0.172	1.08	65.5	4.95	2.23	0.203	1.08	78.8	5.72
<b>WH+15</b>	1.93	0.169	1.06	62.8	4.77	2.13	0.200	1.06	75.5	5.53
<b>WH+10</b>	1.84	0.166	1.04	60.0	4.59	2.04	0.196	1.04	72.2	5.34
<b>WH+5</b>	1.76	0.162	1.02	57.3	4.41	1.95	0.193	1.02	68.9	5.14
<b>WH0</b>	1.67	0.159	1.00	54.6	4.22	1.86	0.189	1.00	65.7	4.94
<b>WH-5</b>	1.59	0.155	0.98	51.8	4.03	1.76	0.185	0.98	62.4	4.73
<b>WH-10</b>	1.51	0.151	0.95	49.1	3.84	1.67	0.181	0.96	59.1	4.52
<b>WH-15</b>	1.42	0.148	0.93	46.4	3.65	1.58	0.176	0.93	55.8	4.30
<b>WH-20</b>	1.34	0.143	0.90	43.7	3.45	1.48	0.171	0.91	52.5	4.08
<b>WH-25</b>	1.26	0.139	0.88	40.9	3.25	1.39	0.167	0.88	49.2	3.85

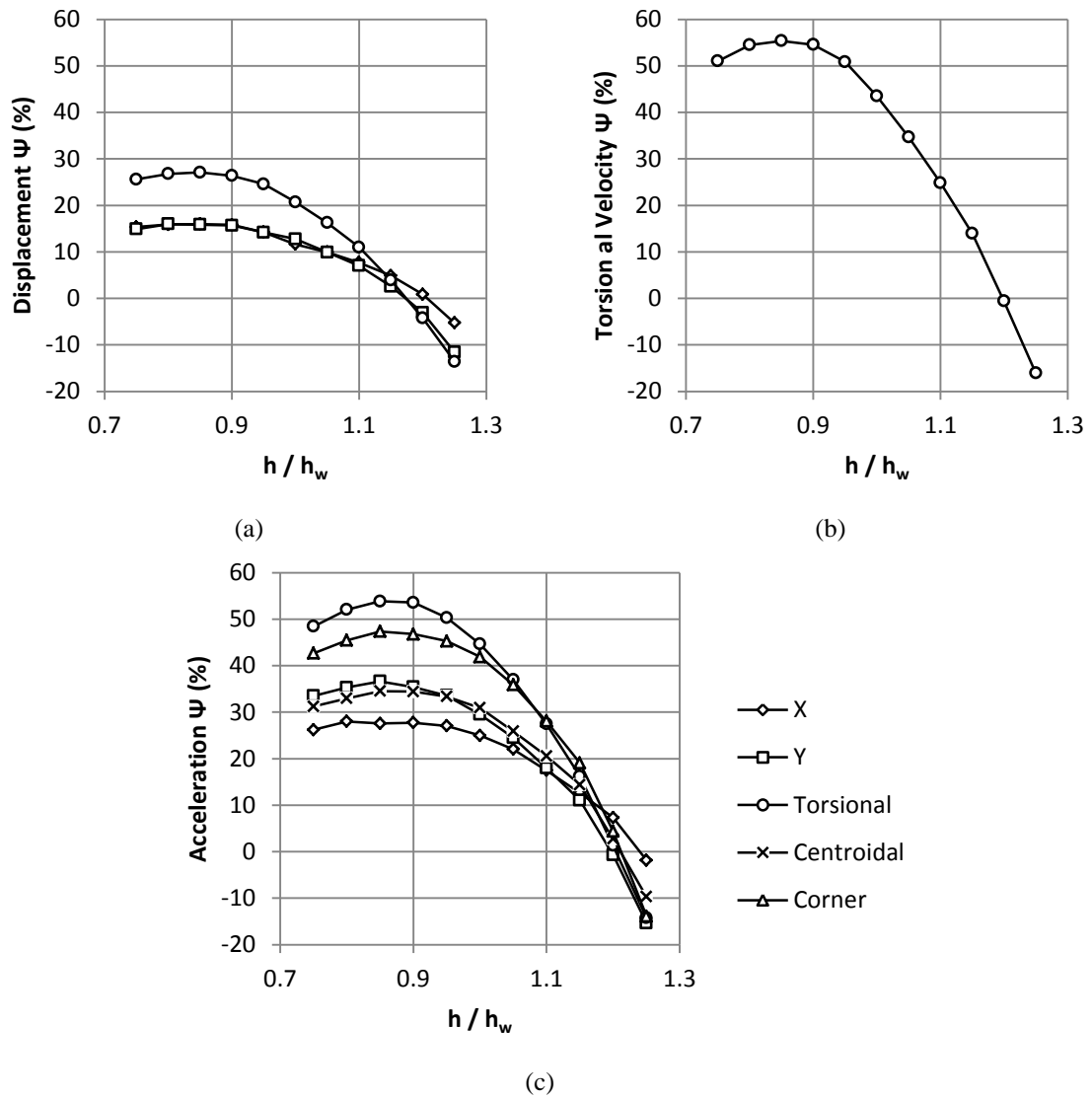


Fig. 9 The effect of water height on the reduction in the (a) displacement, (b) torsional velocity, and (c) acceleration responses of the building

### 6.2 Effect of the amplitude modification factor

The amplitude modification factor (AMF) is introduced in the numerical model to transform the generalized displacement to the real lateral-torsional coupled displacement experienced by the TLD system. For analysis purposes, the multiple tanks are essentially lumped into a single entity, thus removing the complexity of solving each tank separately. The AMF basically transforms the

multiple tank system into a single tank with a generalized water mass equaling the summation of all the tanks. This is possible because the sloshing frequency, damping ratio, and *TLD* property equations remain constant between each tank. The AMF combines each tank into a single entity through a normalized weighted-average of the water mass multiplied by the mode shape at the *TLD* location for each *TLD*. The AMF is dependent on the distance,  $L_\gamma$ , between the CM of the building and the center of mass of each *TLD*. The distance,  $L_\gamma$ , has an upper limit of the perimeter of the building and a lower limit of zero (at the CM). The amplitude modification factor,  $\Phi$ , is numerically tested between these limits. The values are shown in Table 9. By varying the distance between the CM and the tanks, the total generalized water mass,  $M_p$ , changes. This value and the corresponding maximum displacement,  $X_{TLD}$ , used in the *TLD* equations to calculate the properties are also tabulated. The displacement is simply the maximum generalized displacement multiplied by the AMF.

Fig. 10 illustrates the effect of the AMF on the peak hourly response variables. The study reveals a substantial effect due to the change in eccentricity of the tanks. Noticeably, the torsion responses are more sensitive to these changes than the lateral responses. This demonstrates the effectiveness of using the eccentric mass technique to enhance the performance of the *TLD* system in reducing torsional motions. Furthermore, the lateral responses reach a maximum reduction (at the AMF-3 test) with a lower generalized water mass than for the torsional responses (at the AMF+1 test). This confirms the previously discussed limitation on the reduction of the lateral and torsional responses demonstrated between TS-2 and TS-3.

These numerical tests also introduce the influence of the *TLD* mass, frequency, and damping ratio on the response reduction because of the different amplitudes experienced at the CM compared to the perimeter of the floor plan (see Fig. 6 at amplitudes equaling  $X_{TLD}$ ). This study demonstrates that the AMF technique provides an acceptable approach for calculating *TLD* properties.

Table 9 The tests conducted on the amplitude modification factor

Test ID	Mode 1			Mode 2		
	$\Phi$	$M_p$ (kg)	$A$ (mm)	$\Phi$	$M_p$ (kg)	$A$ (mm)
AMF+2	0.00965	77.2	409	0.01066	88.9	147
AMF+1	0.00893	65.9	377	0.00995	77.3	133
AMF0	0.00821	54.6	344	0.00923	65.7	127
AMF-1	0.00742	46.7	301	0.00824	55.4	113
AMF-2	0.00663	38.9	260	0.00725	45.2	98
AMF-3	0.00584	31.1	231	0.00626	35.0	89
AMF-4	0.00505	23.2	212	0.00527	24.7	77
AMF-5	0.00426	15.4	192	0.00428	14.5	70

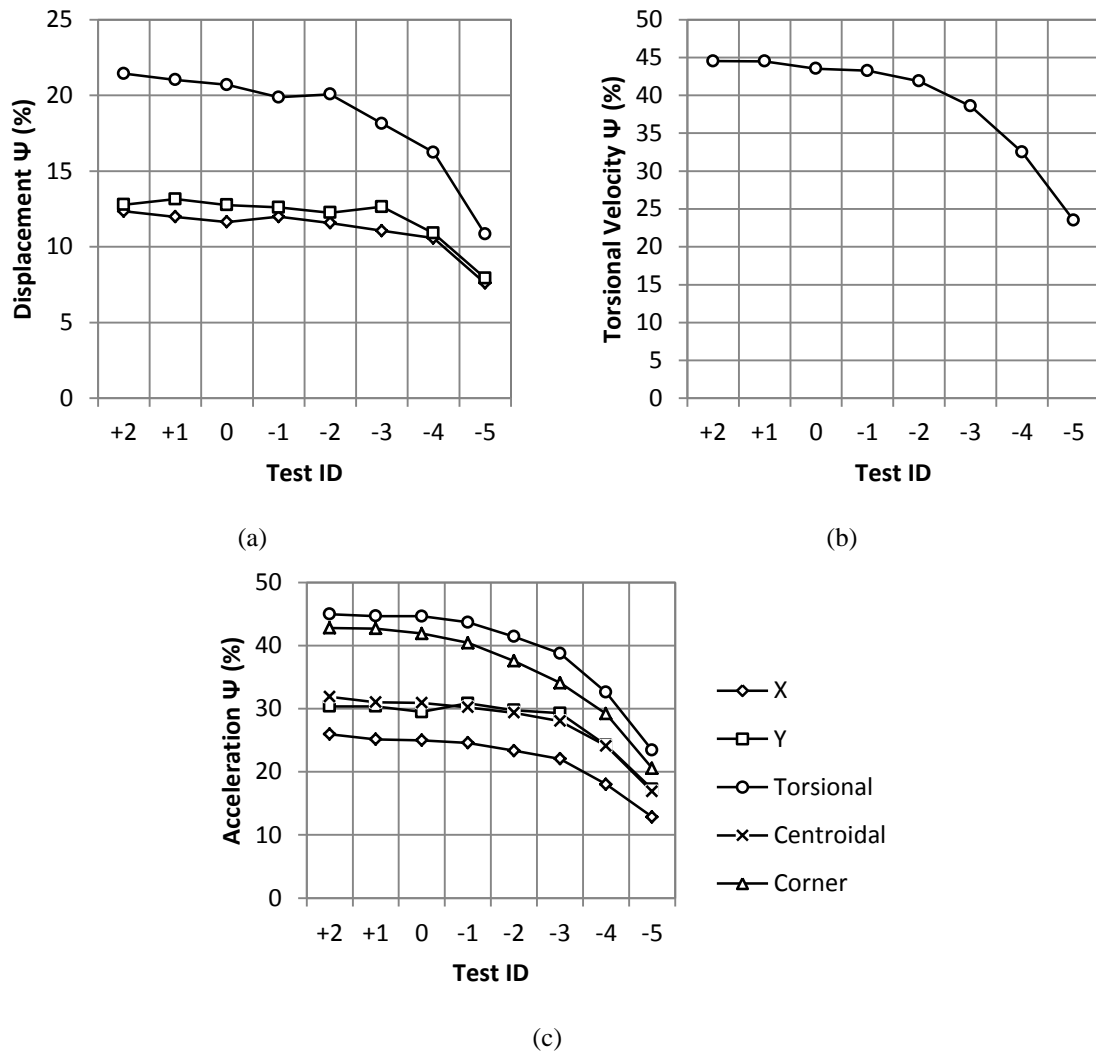


Fig. 10 The effect of the AMF on the reduction in the (a) displacement, (b) torsional velocity, and (c) acceleration responses of the building

### 6.3 Effect of the structural frequencies

The most important parameter for *TLD* design is the tuning ratio. The *TLD* sloshing frequency is well defined; however, the possibility exists that the as-built structural frequencies will deviate from the estimated structural frequencies determined from a computer model by over 15% (Li *et al.* 2007). This leads to a mistuning of the *TLD* system. To investigate this issue, the structural frequencies,  $f_s$ , of the building for the first and second modes are varied separately by  $\pm 15\%$  of the modal frequencies,  $f_1$  and  $f_2$ , obtained from the dynamic analysis. Table 10 summarizes the test parameters.

Table 10 The tests conducted to analyse the effect of the modal frequencies of the building

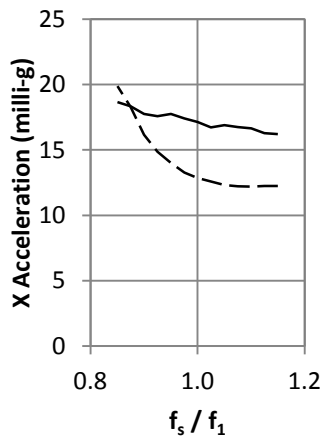
Test ID	Mode 1 Test		Mode 2 Test	
	$f_s$ (Hz)	$\Omega$	$f_s$ (Hz)	$\Omega$
FS+15	0.183	0.870	0.217	0.870
FS+12.5	0.179	0.889	0.212	0.889
FS+10	0.175	0.909	0.208	0.909
FS+7.5	0.171	0.930	0.203	0.930
FS +5	0.167	0.952	0.198	0.952
FS +2.5	0.163	0.976	0.194	0.976
FS0	0.159	1.000	0.189	1.000
FS-2.5	0.155	1.026	0.184	1.026
FS-5	0.151	1.053	0.179	1.053
FS-7.5	0.147	1.081	0.175	1.081
FS-10	0.143	1.111	0.170	1.111
FS-12.5	0.139	1.143	0.165	1.143
FS-15	0.135	1.176	0.160	1.176

Fig. 11 shows the peak hourly responses of the building for the mode 1 test. The responses without a TLD system fluctuate because the frequency content of the wind excites the structure differently. The responses with a TLD system fluctuate less, thereby implying that the TLD system regulates the structural motion regardless of the frequency content of the wind. In addition, the responses with a TLD system remain significantly less than the responses without a TLD system for underestimations of the structural frequency. In this range, the accelerations and torsional velocity remain below the responses without a TLD system because this tuning ratio range is near optimal (slightly less than unity) as described by Eq. (13). Conversely, the effectiveness of the TLD system rapidly decreases if the structural frequency is overestimated. Again, this is related to the tuning ratio departing from the optimal range. In fact, at a structural frequency overestimation of 15%, the TLD system begins to exacerbate the building responses. Notably, the displacements are more sensitive than the accelerations and torsional velocity.

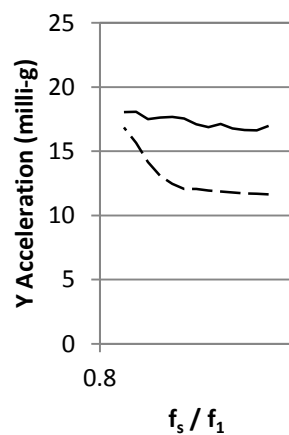
The displacements are far less sensitive to changes in the second mode structural frequency as illustrated in Figs. 12(g)-(i). In addition, the responses in the  $X$  direction are affected far less by the second mode structural frequency than the first mode structural frequency is that. This is because there is minimal dynamic contribution in the  $X$  direction for the second mode, as illustrated in Fig. 1. Similar to the study on the first mode structural frequency, the  $Y$  and  $\theta$  responses are affected by the tuning ratio. However, overestimations of the second mode structural frequency will not be as severe, as illustrated in Fig. 12, because the effect of the mode 1 TLDs on mode 2 is not accounted for in this analysis. In other words, the mode 1 tanks will have a greater

effect on the structure-TLD system for large underestimations of the second mode structural frequency; therefore, likely eliminating the ineffective portion (less than  $f_s/f_2 = 1.0$ ) of the graphs in Fig. 12.

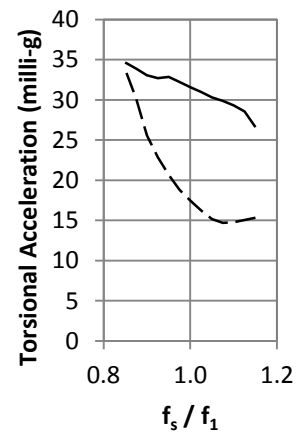
The ability of the TLD system to regulate the structural motions, despite a mistuning, exemplifies the inherent robustness of a well-designed TLD. The TLD system is capable of adapting to a range of tuning ratios, thus increasing the flexibility of the TLD design. This flexibility accommodates fine-tuning after the installation of the TLDs by means of simply adding or removing water. A practical application is fine-tuning the TLDs to match the as-built structural frequencies, which can be determined using in-situ motion monitoring equipment in conjunction with the random decrement technique. A second application involves tuning the TLDs to a range of sloshing frequencies around the structural frequency of interest called a multiple tuned liquid damper (MTLD) system (Fujino and Sun 1993). This ‘mistuning’ improves the effectiveness and robustness of the TLD system by increasing the adaptability to the fluctuating frequency content of the wind and the potentially variable structural frequencies.



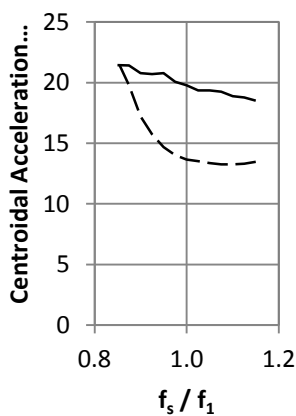
(a)



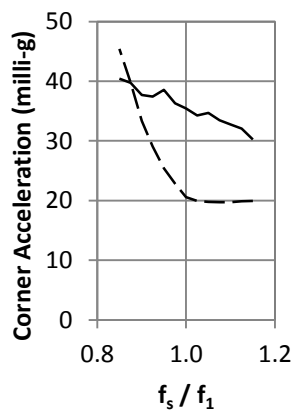
(b)



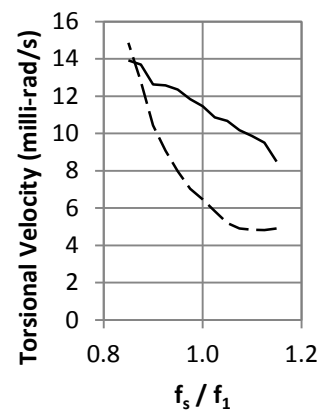
(c)



(d)



(e)



(f)

Continued-

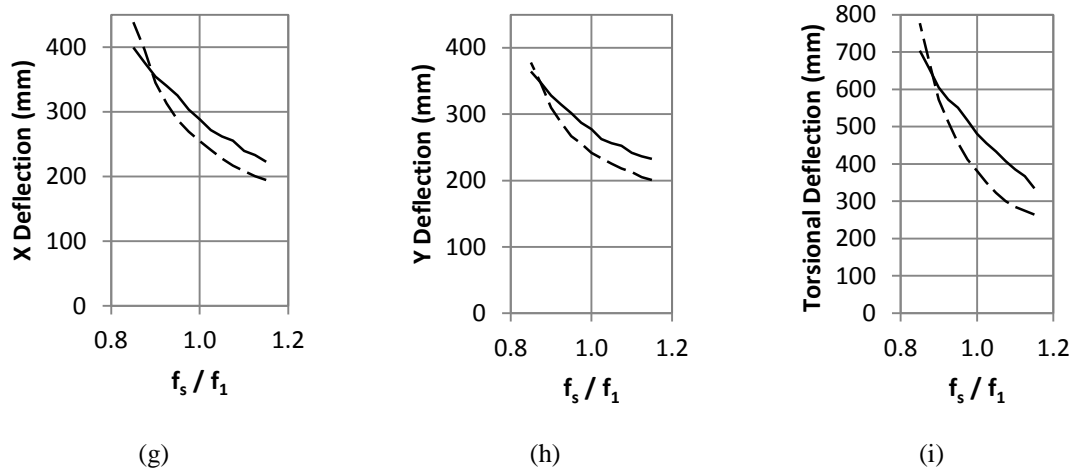


Fig. 11 The peak responses of the building without a TLD system (solid line) and with a TLD system (dashed line) for different first mode structural frequencies

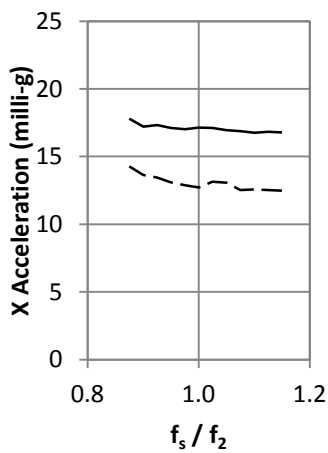
## 7. Conclusions

In this study, three multi-modal TLD systems, denoted as TS-1, TS-2, and TS-3, are described and tested on a lateral-torsional coupled building. The building in this study demonstrates coupled lateral-torsional action for the first three modes. Each TLD system is designed to suppress the first two modes by tuning two sets of tanks to the corresponding structural frequency of the building. In addition, the systems are designed to suppress the torsional motion by placing the tanks around the perimeter of the floor plan to maximize the inertial water mass from the coupled action. The TLD system layouts are chosen to capture a wide range of TLD mass ratios such that TS-2 has a TLD mass ratio approximately twice that of TS-1 and two-thirds that of TS-3. TS-1 uses 1D tanks, TS-2 utilizes 2D tanks, and TS-3 employs two layers of 1D tanks.

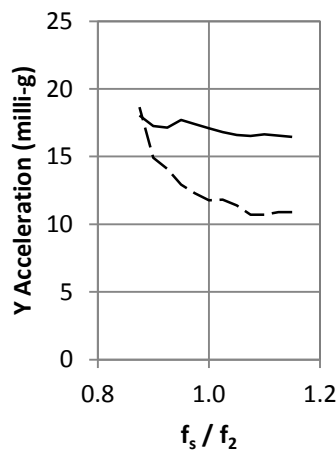
The building with each of the three TLD systems is subjected to wind forces obtained from HFFB tests at the BLWTL at the University of Western Ontario. The results from solving the structure-TLD system demonstrate that the three TLD systems are capable of significantly reducing the motions of the building, specifically the twist. As the water mass is increased, the ability for the TLD to suppress the torsional motion is increased; however, there is an upper limit to the TLD effectiveness with respect to water mass. This appears clearly in comparing the efficiency of the two 1D tanks systems (TS-1 and TS-3). It is noticed that overall the building with TS-3 installed meets the serviceability requirements for human perception of accelerations and almost for the torsional velocity. This is related to the fact that the water mass ratio in TS-3 is higher than TS-1. Furthermore, although the increase in the water mass ratio of TS-2 system, TS-3 design which employs two layers of 1D tanks shows more ability to suppress the torsional motion compared to TS-2 design which utilizes 2D tanks.

To check the practical issues of using a TLD system, a parametric study is conducted on the readily variable properties of the building with TS-3 installed. The first property tested is the water depth inside the TLD, which inherently affects the sloshing frequency and mass of water, simultaneously. The study demonstrates that water heights below the water height that gives a

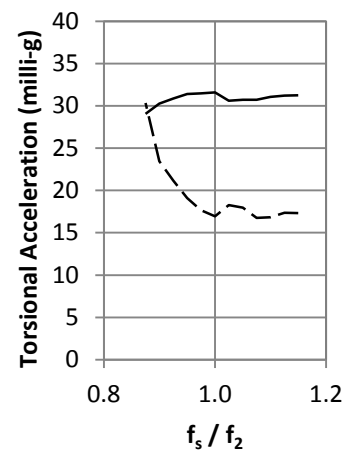
tuning ratio of unity will yield a more effective TLD design. In fact, the change in water height is likely to only benefit the system because it cannot increase, thus maintaining a near optimal efficiency. The second property studied is the amplitude modification factor, which is applied to the numerical model to calculate the physical displacement experienced by the TLD. The study essentially investigates the effect of the eccentricity of the tanks. The results show that there is a response-specific upper limit on the response reduction, which is determined by the amount of generalized water mass. Finally, the effect of varying the first and second structural frequencies on the building response is investigated. The study demonstrates that the frequency content of the wind force causes the building responses to vary without a TLD system; however, the TLD system is capable of reducing the variance and significantly reducing the responses. The responses are dependent on the tuning ratio of the TLD system, thus causing overestimations of the structural frequencies to be severely detrimental to the building; conversely, underestimations increase the TLD effectiveness.



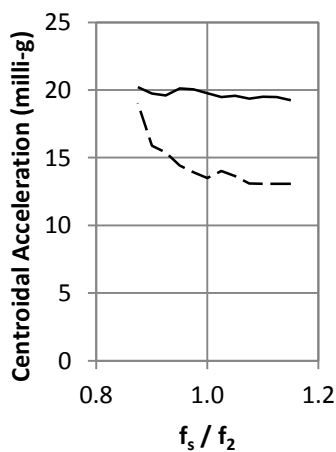
(a)



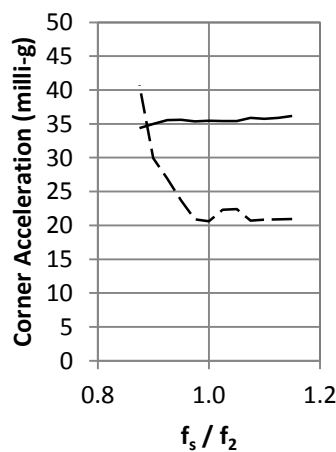
(b)



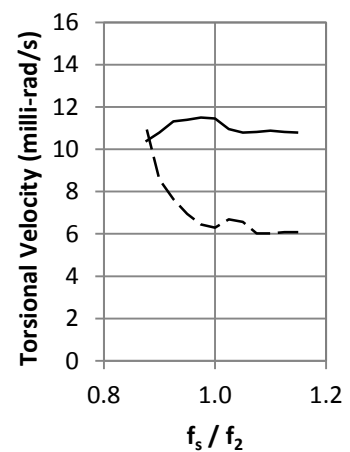
(c)



(d)



(e)



(f)

Continued-

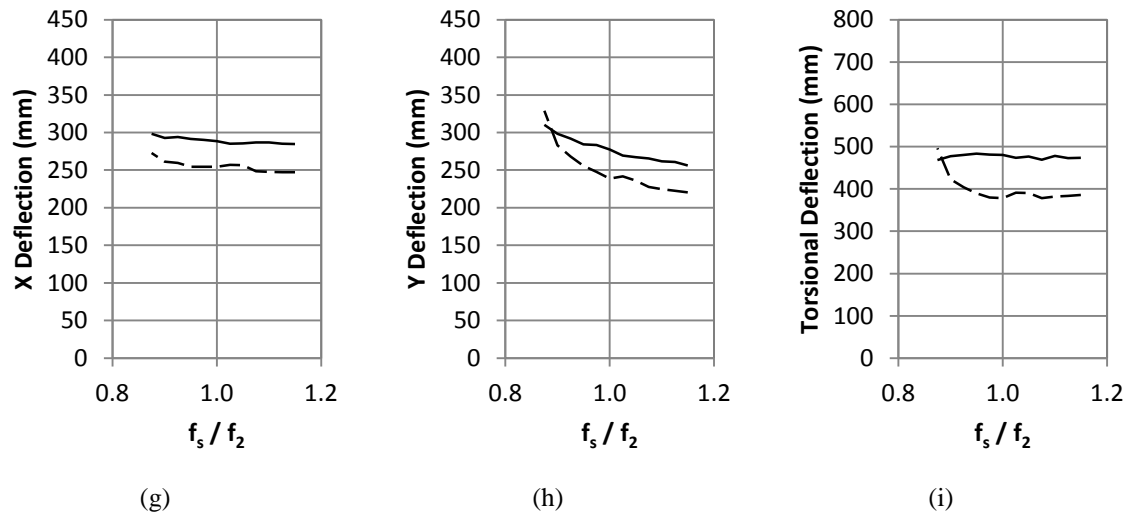


Fig. 12 The peak responses of the building without a TLD system (solid line) and with a TLD system (dashed line) for different second mode structural frequencies

Overall, the TS-3 design for the building is an effective and robust alternative for controlling the coupled lateral-torsional structural motions. To improve the TLD design, an MTLTD system can be used to capture a range of frequencies excited by the wind loading. This is still a relatively new concept and is an area for future research. In addition, as a means to increase the robustness of a TLD system, a post-construction dynamic survey of the building should be carried-out and the TLD system should be fine-tuned to match the as-built structural frequencies. Furthermore, placing water height monitoring devices in the TLDs will significantly reduce the chance of an undesirable mistuning.

## Acknowledgments

The research described in this paper was financially supported by the Ontario Graduate Scholarship (OGS). The authors would like to express their gratitude to Eric Ho from the Boundary Layer Wind Tunnel Laboratory (BLWTL) at Western University for his valuable discussions of the research conducted in this study.

## References

- Fediw, A.A., Isyumov, N. and Vickery, B.J. (1995), "Performance of a tuned sloshing water damper", *J. Wind Eng. Ind. Aerod.*, **57**(2-3), 237-247.
- Fujino, Y. and Sun, L.M. (1993), "Vibration control by multiple tuned liquid dampers (MTLDs)", *J. Struct. Eng. - ASCE*, **119**(12), 3482-3502.
- Hansen, R.J., Reed, J.W. and Vanmarcke, E.H. (1973), "Human response to wind-induced motion of buildings", *J. Struct. Div.*, **99**(7), 1589-1605.
- Isyumov, N. (1994), "Criteria for acceptable wind-induced motions", *Proceedings of the 12th ASCE*

- Structures Congress*, Atlanta.
- Kareem, A. (1990), "Reduction of wind induced motion utilizing a tuned sloshing damper", *J. Wind Eng. Ind. Aerod.*, **36**, 725-737.
- Koh, C.G., Mahatma, S. and Wang, C.M. (1995). "Reduction of structural vibrations by multiple-mode liquid dampers", *Eng. Struct.*, **17**(2), 122-128.
- Lam, K.M. and Li, A. (2009), "Mode shape correction for wind-induced dynamic responses of tall buildings using time-domain computation and wind tunnel tests", *J. Sound Vib.*, **322**(4-5), 740-755.
- Li, H.N., Jia, Y. and Wang, S.Y. (2004), "Theoretical and experimental studies on reduction for multi-modal seismic responses of high-rise structures by tuned liquid dampers", *J. Vib. Control*, **10**(7), 1041-1056.
- Li, Q.S., Xiao, Y.Q., Fu, J.Y. and Li, Z.N. (2007), "Full-scale measurements of wind effects on the Jin Mao building", *J. Wind Eng. Ind. Aerod.*, **95**(6), 445-466.
- Lieblein, J. (1974), *Efficient methods of extreme-value methodology*, Report No. NBSIR 74-602, Institute for Applied Technology, Department of Commerce. Washington, D.C., National Bureau of Standards.
- Modi, V.J., Welt, F. and Irani, M.B. (1990), "On the suppression of vibrations using nutation dampers", *J. Wind Eng. Ind. Aerod.*, **33**(1-2), 273-282.
- Pagnini, L.C. and Solari, G. (1998), "Serviceability criteria for wind-induced acceleration and damping uncertainties", *J. Wind Eng. Ind. Aerod.*, **74-76**, 1067-1078.
- Rahman, M. (2007), *The Use of Tuned Liquid Dampers to Enhance the Seismic Performance of Concrete Rigid Frame Buildings*, Ph. D. Thesis. London, Ontario, Canada: The University of Western Ontario.
- Reed, D., Yeh, H., Yu, J. and Gardarsson, S. (1998), "Tuned liquid dampers under large amplitude excitation", *J. Wind Eng. Ind. Aerod.*, **74-76**, 923-930.
- Singh, M.P., Singh, S. and Moreschi, L.M. (2002), "Tuned mass dampers for response control of torsional buildings", *Earthq. Eng. Struct. D.*, **31**(4), 749-769.
- Sun, L.M. and Fujino, Y. (1994), "A semi-analytical model for tuned liquid damper (TLD) with wave breaking", *J. Fluid. Struct.*, **8**(5), 471-488.
- Sun, L.M., Fujino, Y., Chaiseri, P. and Pacheco, B.M. (1995), "The properties of tuned liquid dampers using a TMD analogy", *Earthq. Eng. Struct. D.*, **24**(7), 967-976.
- Tait, M.J., El Damatty, A.A. and Isyumov, N. (2004a), "Testing of tuned liquid damper with screens and development of equivalent TMD analogy", *Wind Struct.*, **7**(4), 215-234.
- Tait, M.J., Isyumov, N. and El Damatty, A.A. (2004b), "The efficiency and robustness of a uni-directional tuned liquid damper and modelling with an equivalent TMD", *Wind Struct.*, **7**(4), 235-250.
- Tait, M.J., El Damatty, A.A., Isyumov, N. and Siddique, M.R. (2005a), "Numerical flow models to simulate tuned liquid dampers (TLD) with slat screens", *J. Fluid. Struct.*, **20**(8), 1007-1023.
- Tait, M.J., El Damatty, A.A. and Isyumov, N. (2005b), "An investigation of tuned liquid dampers equipped with damping screens under 2D excitation", *Earthq. Eng. Struct. D.*, **34**, 719-735.
- Tait, M.J., Isyumov, N. and El Damatty, A.A. (2007), "Effectiveness of a 2D TLD and its numerical modeling", *J. Struct. Eng. - ASCE*, **133**(2), 251-263.
- Tait, M.J. (2008a), "Modelling and preliminary design of a structure-TLD system", *Eng. Struct.*, **30**(10), 2644-2655.
- Tait, M.J., Isyumov, N. and El Damatty, A.A. (2008b), "Performance of tuned liquid dampers", *J. Eng. Mech. - ASCE*, **134**(5), 417-427.
- Tamura, Y., Kohsaka, R., Nakamura, O., Miyashita, K.I. and Modi, V.J. (1996), "Wind-induced responses of an airport tower - efficiency of tuned liquid damper", *J. Wind Eng. Ind. Aerod.*, **65**(1-3), 121-131.
- Tschanz, T. (1982), *The Base Balance Measurement Technique and Applications to Dynamic Wind Loading of Structures*, Ph.D. Thesis. London, Ontario, Canada: The University of Western Ontario.
- Tse, K.T., Kwok, K.C., Hitchcock, P.A., Samali, B. and Huang, M.F. (2007), "Vibration control of a wind-excited benchmark tall building with complex lateral-torsional modes of vibration", *Adv. Struct. Eng.*, **10**(3), 283-304.
- Tse, K.T., Hitchcock, P.A. and Kwok, K.C. (2009), "Mode shape linearization for HFBB analysis of wind-excited complex", *Eng. Struct.*, **31**(3), 675-685.
- Ueng, J.M., Lin, C.C. and Wang, J.F. (2008), "Practical design issues of tuned mass dampers for torsionally

- coupled buildings under earthquake loadings”, *Struct. Des. Tall Special Build.*, **17**, 133-165.
- Warnitchai, P. and Pinkaew, T. (1998), “Modelling of liquid sloshing in rectangular tanks with flow-dampening devices”, *Eng. Struct.*, **20**(7), 593-600.
- Xu, Y.L., Kwok, K.C. and Samali, B. (1992), “Torsion response and vibration suppression of wind-excited buildings”, *J. Wind Eng. Ind. Aerod.*, **41-44**, 1997-2008.
- Yip, D.Y. (1995). *Wind-Induced Dynamic Response of Tall Buildings with Coupled 3D Modes of Vibration*, Ph.D. Thesis, Auckland, New Zealand: University of Auckland.
- Yip, D.Y. and Flay, R.G. (1995), “A new force balance data analysis method for wind response predictions of tall buildings”, *J. Wind Eng. Ind. Aerod.*, **54-55**, 457-471.
- Zhou, Y., Gu, M. and Xiang, H. (1999b), “Along-wind static equivalent wind loads and responses of tall buildings. Part II: effects of mode shapes”, *J. Wind Eng. Ind. Aerod.*, **79**, 151-158.